Pergamon

SCIENCE DIRECT®

Tetrahedron 59 (2003) 7291–7299

TETRAHEDRON

Synthesis, properties, and oxidizing function of 6-substituted 7,9-dimethylcyclohepta[*b*]pyrimido[5,4-*d*]pyrrole-8(7*H*),10(9*H*)-dionylium tetrafluoroborates

Shin-ichi Naya and Makoto Nitta*

Department of Chemistry, School of Science and Engineering, Waseda University, Shinjuku-ku, Tokyo 169-8555, Japan

Accepted 24 July 2003

Abstract—Uracil-annulated heteroazulenes, 6-substituted 7,9-dimethylcyclohepta[*b*]pyrimido[5,4-*d*]pyrrole-8(7*H*),10(9*H*)-dionylium tetrafluoroborates **7a**,**b**·BF_4^-, which are the isoelectronic compounds of 5-dezazaflavin, were synthesized. X-Ray crystal analysis and MO calculations were carried out to clarify the structural characteristics of **7a**,**b**·BF_4^-. The stability of cations **7a**,**b** is expressed by the pK_{R+} values which were determined spectrophotometrically to be 10.9 and 11.2, respectively. The electrochemical reduction of **7a**,**b** exhibited high reduction potentials at −0.84 and −0.87 (V vs $Ag/AgNO_3$) upon cyclic voltammetry (CV). A good linear correlation between the pK_{R+} values and reduction potentials ($E1_{red}$) of **7a**,**b**·BF_4^- and reference compounds **4**·BF_4^- and **5**·BF_4^- was obtained. In a search of the reactivity, reactions of **7a**,**b**·BF_4^- with some nucleophiles, hydride and diethylamine, were carried out to clarify that the introduction of nucleophiles to give regio-isomers is dependent on the nucleophile. The photo-induced oxidation reactions of **7a**,**b**·BF_4^- toward some alcohols under aerobic conditions were carried out to give the corresponding carbonyl compounds in more than 100% yield [based on compounds **7a**,**b**·BF_4^-], suggesting the oxidizing function of **7a**,**b**·BF_4^- toward alcohols in the autorecycling process.

1. Introduction

Flavin plays an important role as co-factor in a wide variety of biological redox reactions.[1] Dehydrogenation reactions represent a major family of processes mediated by a subclass of flavoenzymes known as oxidases. Included in this group are the oxidative transformations of alcohols to carbonyl compounds, of amines to imines, and of fatty acid esters to their α,β-unsaturated analogs.[2] The importance of fused uracils, which are common sources for the development of new potential therapeutic agents, is also well known.[3,4] Among these, 5-deazaflavin **1a** has been studied extensively in both enzymatic[5] and model systems[6,7] in the hope of providing mechanistic insight into flavin-catalyzed reactions. In addition, 5-deaza-10-oxaflavin **1b** [2*H*-chromeno[2,3-*d*]pyrimidine-2,4(3*H*)-dione][8] and 5-deaza-10-thiaflavin **1c** [1-benzothiopyrano[2,3-*d*]pyrimidine-2,4(3*H*)-dione][9] (Fig. 1), in which the nitrogen atom of 5-deazaflavin **1a** is replaced by an oxygen and a sulfur, respectively, have been synthesized and found to possess a function to oxidize alcohols to the corresponding carbonyl compounds. In these reports, compounds **1a**–**c** have been considered as models not only of flavin but also of NAD. On the basis of the above observations, we have previously studied convenient preparations of 6,9-disubstituted cyclohepta[*b*]pyrimido[5,4-*d*]pyrrole-8(6*H*),10(9*H*)-diones **2a**,**b**[10] and 9-methylcyclohepta[*b*]pyrimido[5,4-*d*]furan-8,10(9*H*)-dione **3**,[11] which are structural isomers of 5-deazaflavin **1a** and 5-deaza-10-oxaflavin **1b**, and their functions in oxidizing some alcohols to the corresponding carbonyl compounds. In relation to the studies, we have

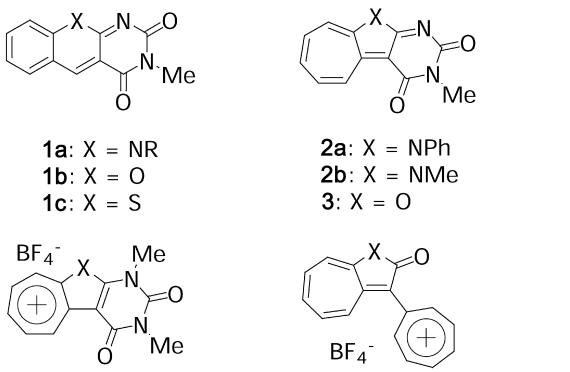

Figure 1.

Keywords: 7,9-dimethylcyclohepta[*b*]pyrimido[5,4-*d*]pyrrole-8(7*H*),10(9*H*)-dionylium tetrafluoroborates; pK_{R+}; reduction potential; photo-induced oxidation reaction.

* Corresponding author. Tel.: +81-3-5286-3236; fax: +81-3-3208-2735; e-mail: nitta@waseda.jp

0040–4020/$ - see front matter © 2003 Published by Elsevier Ltd.
doi:10.1016/S0040-4020(03)01150-5

recently reported the synthesis, properties, and reactivity of 7,9-dimethylcyclohepta[*b*]pyrimido[5,4-*d*]furan-8(7*H*),10(9*H*)-dionylium tetrafluoroborate **4**·BF_4^-[12,13] and its sulfur analogue **5**·BF_4^-[14] (Fig. 1) as well as the photo-induced autorecycling oxidizing reactions of **4**·BF_4^- and **5**·BF_4^- toward some alcohols. This type of oxidizing functions of non-alternant heteroaromatic compounds, such as the heteroazulenes, has not been previously reported. Thus, the uracil-annulated heteroazulenes are extremely interesting from the aspect of exploration of novel functions of non-alternant heteroaromatic compounds.

On the other hand, we have studied the synthesis and properties of heteroazulene-substituted methyl cations[15–19] and tropylium ions **6a**–**d**·BF_4^-.[20] In the studies, we clarified that the reduction potentials and pK_{R+} values of these cations exhibited a good linear correlation, and they were highly dependent on the heteroatoms in the heteroazulene moiety. Thus, the properties of the nitrogen analogue of **4**·BF_4^- and **5**·BF_4^- are interesting. We have now studied the synthesis and properties of 6-substituted 7,9-dimethylcyclohepta[*b*]pyrimido[5,4-*d*]pyrrole-8(7*H*),10(9*H*)-dionylium tetrafluoroborates **7a**,**b**·BF_4^- (Scheme 1). Their structural details and reactivity as well as the photo-induced oxidizing reaction of **7a**,**b**·BF_4^- toward some alcohols were investigated. We report herein the results in detail.

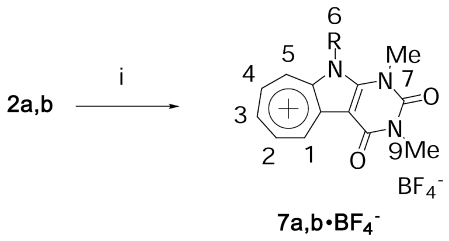

Scheme 1. *Reagents and conditions*: (i) (a) MeI, $(CH_2Cl)_2$, 120°C, 12 h; (b) 42% aq. HBF_4, Ac_2O, 0°C, 1 h.

2. Results and discussion

2.1. Synthesis and properties

Preparation of cations **7a**,**b**·BF_4^- was easily accomplished by the methylation of **2a**,**b**[10] and subsequent exchange of the counter-anion. Although pyridine derivatives react easily with MeI at rt to give pyridinium cations,[21] compounds **2a**,**b** did not react with MeI in CH_2ClCH_2Cl at rt for 48 h, and **2a**,**b** were recovered quantitatively. Thus, reactions of **2a**,**b** with excess MeI in CH_2ClCH_2Cl at 120°C for 12 h and subsequent anion exchange reaction using aq. HBF_4 in Ac_2O afforded **7a**,**b**·BF_4^- in 98 and 83% yields, respectively (Scheme 1). The strong reaction conditions are required probably due to the steric hindrance experienced with the N6-substituent and the N7-Me group (vide infra). The cations **7a**,**b**·BF_4^- were fully characterized on the basis of NMR, IR, UV–vis, mass spectral data as well as elemental analyses and X-ray structure analyses. Mass spectra of the salts **7a**,**b**·BF_4^- ionized by FAB exhibited the correct M^+-BF_4 ion peaks, which are indicative of the cationic structure of these compounds. The characteristic

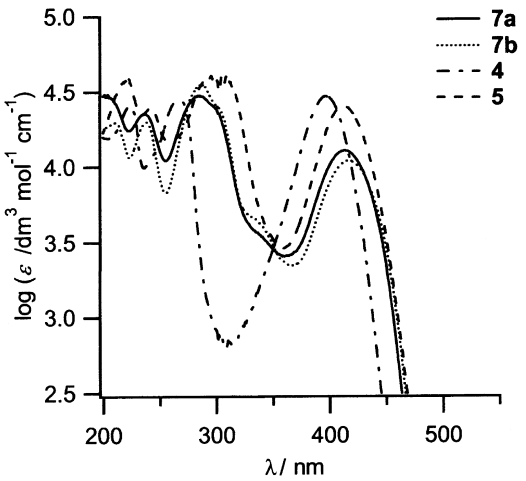

Figure 2. UV–vis spectra of **7a**,**b** in CH_3CN.

bands for the counter ion BF_4^- were observed at 1082 and 1084 cm^{-1} in the IR spectra of **7a**,**b**·BF_4^-, respectively. In the ^1H NMR spectra, the proton signals on the seven-membered ring of **7a**,**b**·BF_4^- (**7a**: δ 8.27–9.97; **7b**: δ 8.46–9.89) appeared at lower-field than those of **2a**,**b** (**2a**: δ 7.44–9.37; **2b**: δ 7.69–9.26).[10] These features also support the cationic nature of the compounds. In addition, the proton signal of N7-Me of **7a**·BF_4^- (δ 3.14) is remarkably shifted to higher-field as compared with those of N7-Me of **4**·BF_4^- (δ 3.73),[12] **5**·BF_4^- (δ 3.76),[14] and **7b**·BF_4^- (δ 3.94), suggesting that N7-Me of **7a**·BF_4^- is located within a shielding region of the phenyl group. This feature is confirmed by X-ray structure analysis (vide infra). UV–vis spectra of **7a**,**b** in acetonitrile are shown in Figure 2, together with those of **4**[12] and **5**.[14] While the spectra of **7a**,**b** are a different shape from that of **4**, the spectra of **7a**,**b** and **5** are similar and the longest wavelength absorption maxima show slight shifts (**7a**, 414 nm; **7b**, 417 nm; **5**, 414 nm).

The single crystals of **7a**,**b**·BF_4^- were obtained by recrystallization from CH_3CN/Et_2O and CH_3CN/AcOEt, respectively. Thus, in order to clarify the structural details, X-ray structure analyses were carried out and the ORTEP drawings of **7a**,**b**·BF_4^- are shown in Figure 3. The π-system of compound **7a**·BF_4^- has a nearly planar structure. The plane of the phenyl group is twisted 85° against the plane of the π-system probably due to steric hindrance between the phenyl group and the N7-Me group. Similarly, compound **7b**·BF_4^- has a nearly planar structure and the N6-Me and the N7-Me groups deviated from the plane due to the steric hindrance between them. These steric effects are considered to require vigorous conditions of the methylation of **2a**,**b** (vide supra). The selected bond lengths are summarized in Table 1 (the numbering is shown in Figure 4). On both compounds **7a**,**b**·BF_4^-, the bond lengths of C1–C2, C3–C4, and C5–C5a are shorter than those of C2–C3, C4–C5, C5a–C10b, and C10b–C1. This fact suggests the existence of bond alternation in the seven-membered ring, as shown in **7a**,**b**-B and **7a**,**b**-C. In addition, since the bond length of C5a–N6 is longer than that of N6–C6a, the contribution of **7a**,**b**-D seems to be less important. MO calculations of **7a**,**b** were carried out by the 6-31G* basis set of the MP2 levels[22] and the selected bond lengths are also summarized in Table 1. The bond length alternations obtained by MO

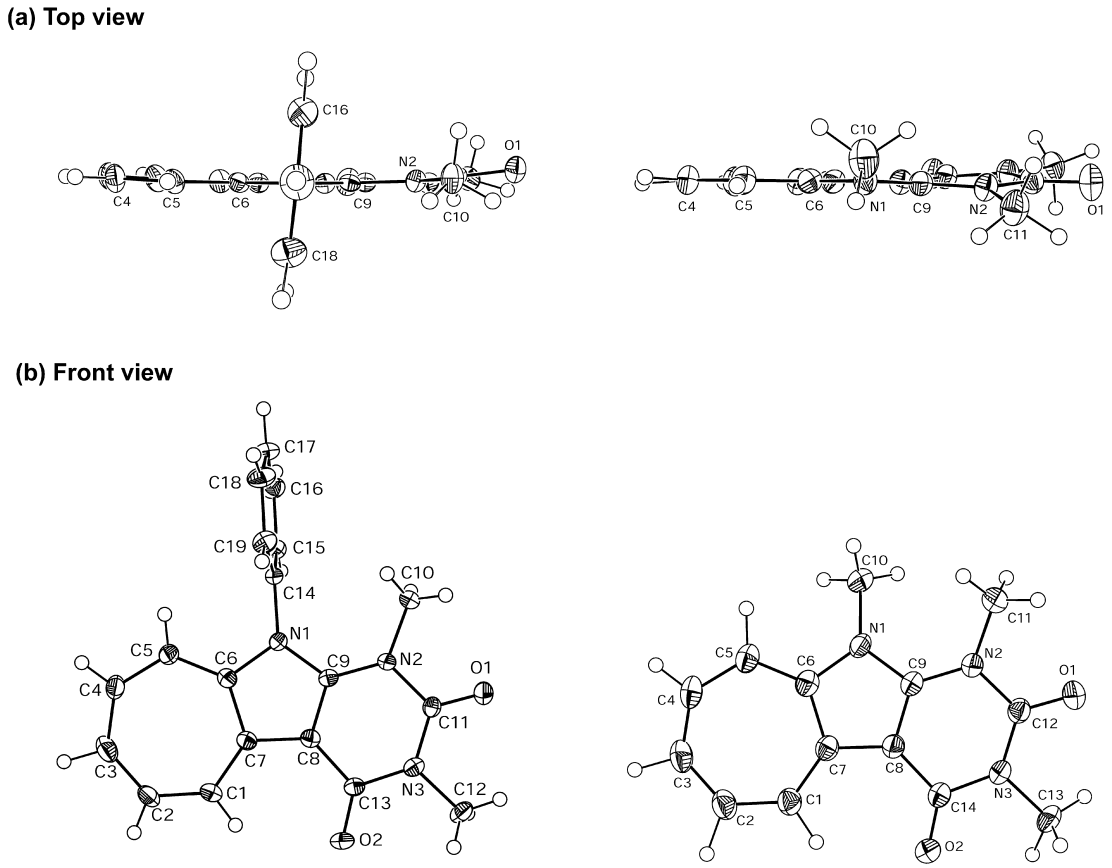

Figure 3. ORTEP drawings of **7a**,**b**·BF_4^- with thermal ellipsoid plot (50% probability).

Table 1. Bond lengths of **7a**,**b**·BF_4^- obtained by X-ray structure analysis and MO calculation

Cation	Method	Bond length[a] (Å)											
		C1–C2	C2–C3	C3–C4	C4–C5	C5–C5a	C5a–C10b	C10b–C1	C5a–N6	N6–C6a	C6a–N7	C6a–C10a	C10a–C10b
7a	X-ray	1.39	1.40	1.39	1.40	1.37	1.45	1.40	1.40	1.38	1.34	1.40	1.40
7a	MP2/6-31G*	1.39	1.41	1.39	1.40	1.39	1.45	1.41	1.40	1.38	1.35	1.40	1.41
7b	X-ray	1.39	1.38	1.38	1.40	1.38	1.44	1.39	1.39	1.37	1.34	1.39	1.41
7b	MP2/6-31G*	1.38	1.40	1.38	1.39	1.39	1.46	1.40	1.42	1.40	1.37	1.44	1.42

[a] The numbering is shown in Figure 4.

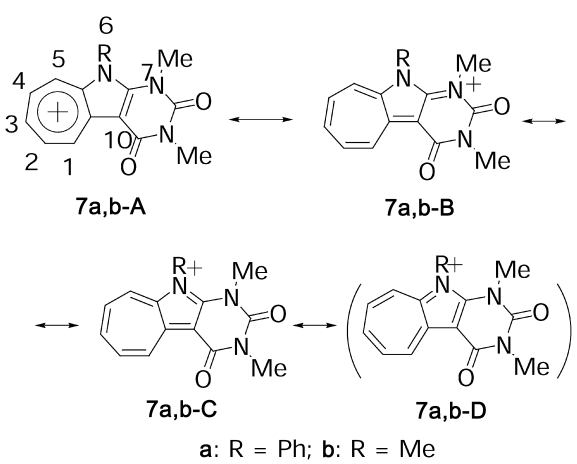

Figure 4.

calculation for **7a**,**b** are very similar to those obtained by X-ray analyses. These remarkable bond alternations of **7a**,**b** are also observed for the cations **5**·BF_4^-[13] and derivatives of **4**·BF_4^-.[14]

The affinity of the carbocation towards hydroxide ions, expressed by the pK_{R+} value, is the most common criterion of carbocation stability.[23] The pK_{R+} values of cations **7a**,**b** were determined spectrophotometrically in buffer solutions prepared in 50% aqueous CH_3CN (Section 4) and are summarized in Table 2, along with those of reference compounds **4**,[12] **5**,[14] and tropylium ion **8**.[24] The pK_{R+} values of **7a**,**b** were determined to be 10.9 and 11.2 respectively; these are much larger than those of **4**, **5**, and **8**. In addition, the pK_{R+} values are larger in the order **5**<**4**≪**7a**<**7b**. Thus, the electron-donating ability of the heteroatom groups on these cations is larger in the order S<O≪NPh<NMe. This feature is similar to that of the

Table 2. pK_{R+} Values and reduction potentials of cations **7a**,**b** and reference compounds **4**, **5**, and tropylium ion **8**

Compound	pK_{R+}	Reduction potential, $E1_{red}$ (V)
7a	10.9	−0.84
7b	11.2	−0.87
4[a]	ca. 6.0	−0.58
5[b]	5.1	−0.53
8[c]	3.9	−0.51

V vs. $Ag/AgNO_3$; cathodic peak potential. Salts **7a**,**b**·BF_4^- were used for the measurement.
[a] Ref. 12.
[b] Ref. 14.
[c] Ref. 24.

cations **6a**–**d** (**6a**, pK_{R+} 3.2<**6b**, pK_{R+} 3.8≪**6c**, pK_{R+} 5.3<**6d**, pK_{R+} 5.7).[20]

The reduction potentials of **7a**,**b** were determined by cyclic voltammentry (CV) in CH_3CN. The reduction waves of **7a**,**b** were irreversible under the conditions of the CV measurements; the peak potentials are summarized in Table 2, together with those of the reference compounds **4**,[12] **5**,[14] and **8**.[24] The $E1_{red}$ of **7a**,**b** are more negative by 0.33 and 0.36 V than that of tropylium ion **8**. The irreversible nature is probably due to the formation of tropyl radicals and their dimerization. This reduction behavior seems to be a typical property of tropylium ions.[25] The reduction potentials ($E1_{red}$) of **4**, **5**, and **7a**,**b** are in a wide range (−0.53 to −0.87 V), suggesting that uracil-annulated heteroazulenes are useful as molecular catalysts endowed with variable oxidizing ability.

The pK_{R+} values of cations **4**, **5**, and **7a**,**b** are plotted against the $E1_{red}$ values of these cations (Fig. 5). The units of $E1_{red}$ and pK_{R+} values were converted to the kJ/mol [$-96.5\times E1_{red}$/V and $5.7\times(pK_{R+}-14)$].[16,20] A good linear correlation line was obtained, and the slope and *y*-intercept of this regression line were 1.09 and −106.89, respectively (correlation coefficient=0.999). We have previously reported a similar correlation line obtained for cations **6a**–**d**, and the slope and *y*-intercept were obtained as 0.72 and −93.94, respectively.[20] The slope of the regression line of cations **4**, **5**, and **7a**,**b** is larger than that of cations **6a**–**d**. Furthermore, the value is larger than 1.0, suggesting that the more stable cation gives a more stable radical in single-electron reduction of **4**, **5**, and **7a**,**b**.[16] The uracil-moiety is an electron-withdrawing group and the large electron-donating ability of the heteroatom on the five-membered ring would stabilize the radical species to greater extent by the captodative effect (Scheme 1).[26]

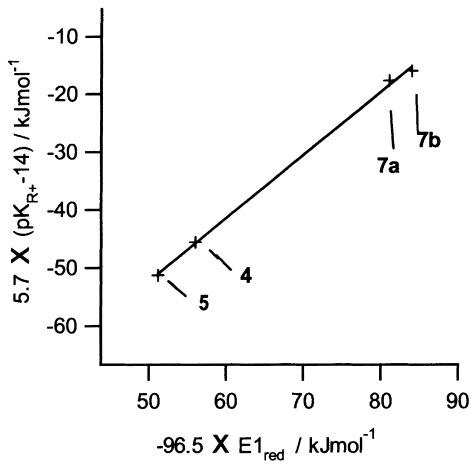

Figure 5. Plot of pK_{R+} values against $E1_{red}$ of **4**, **5**, **7a**, and **7b**.

2.2. Reactivity of 7a,b·BF_4^-

In the reaction of **4**·BF_4^- and **5**·BF_4^- with some nucleophiles, the reaction site of the cations showed remarkable difference depending on the nucleophile and the heteroatom on the five-membered ring. Thus, in order to clarify the reactivity of cations **7a**,**b**·BF_4^-, the reactions of **7a**,**b**·BF_4^- with some nucleophiles were carried out. The results are summarized in Table 3. Reduction of **7a**,**b**·BF_4^- with $NaBH_4$ in CH_3CN afforded mixtures of three compounds **9a**–**11a** and **9b**–**11b**, and the mixtures are oxidized by DDQ to regenerate **7a**,**b**·BF_4^- in good yield (Scheme 2, Table 3, entries 1 and 2). Since the regio-isomers could not be separated, the structural assignments were based on NMR, IR, mass spectral data as well as elemental analyses of the mixtures. The ^1H NMR spectra of the mixtures of each regio-isomer could be assigned by using the H–H COSY spectra, and they are summarized in Table 4. Although steric hindrance of the 5-position of **7a**,**b**·BF_4^- would be greater as compared with that of the 3-position, the ratios of 5-adducts **11a**,**b** are higher than those of 1- and 3-adducts. Furthermore, the ratios of 5-adduct became higher in the order **4**·BF_4^- (59%)<**5**·BF_4^- (61%)<**7a**·BF_4^- (68%)<**7b**·BF_4^- (81%), however, details are unclear at the present stage.

The reaction of **4**·BF_4^- with diethylamine afforded 5a-adduct, which underwent ring-opening reaction, while the reaction of **5**·BF_4^- with diethylamine afforded a mixture of 3-adduct and 5-adduct. Thus, reactions of **7a**,**b**·BF_4^- with diethylamine were monitored by NMR spectroscopy in CD_3CN. The diethylamine addition of **7a**,**b**·BF_4^- occurred at only the 3-position to afford **12a**,**b** (Scheme 3, Table 3, entries 3 and 4). Although compounds **12a**,**b** are stable in dilute solution (CH_3CN), they decompose during

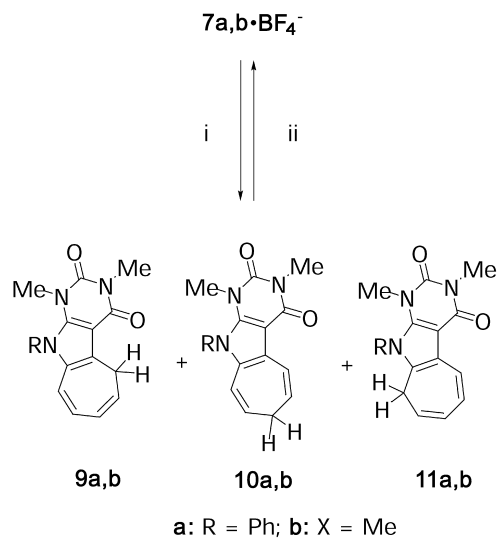

Scheme 2. *Reagents and conditions*: (i) $NaBH_4$, CH_3CN, rt, 1 h; (ii) (a) DDQ, CH_2Cl_2, rt, 1 h; (b) 42% aq. HBF_4, Ac_2O, 0°C, 1 h.

Table 3. Results for the reactions of **7a**,**b**·BF_4^- with some nucleophiles

Entry	Cation	Nucleophile	Product (combined yield)	Ratio of adduct			Regeneration of cation, **7a,b**·BF_4^- (%)
				1-adduct	3-adduct	5-adduct	
1	**7a**·BF_4^-	$NaBH_4$	**9a**–**11a** (70%)	**9a** (25)	**10a** (7)	**11a** (68)	100
2	**7b**·BF_4^-	$NaBH_4$	**9b**–**11b** (96%)	**9b** (15)	**10b** (4)	**11b** (81)	100
3	**7a**·BF_4^-	Et_2NH	**12a** (100%)		**12a** (100)		100
4	**7b**·BF_4^-	Et_2NH	**12b** (100%)		**12b** (100)		100

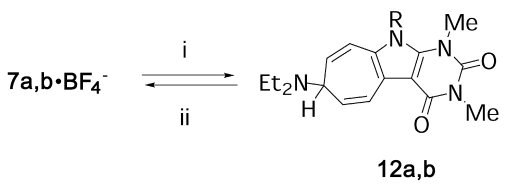

Scheme 3. *Reagents and conditions*: (i) Et_2NH, CD_3CN, rt, 0.5 h; (ii) 42% aq. HBF_4, Ac_2O, 0°C, 1 h.

cyclohexanone. The results are summarized in Table 5. Direct irradiation of the alcohols in the absence of **7a**,**b**·BF_4^- (named 'blank') gives the corresponding carbonyl compounds in low to modest yields. Thus, the yields are calculated by subtraction of the 'blank' yield from the yield of the carbonyl compound in the presence of **7a**,**b**·BF_4^-. More than 100% yields are obtained [based on compounds **7a**,**b**·BF_4^-] (Table 5, entries 1–4), and thus, autorecycling oxidation clearly proceeds.

Table 4. ^1H NMR spectral data (500 MHz) of addition products **9a**–**11a**, **9b**–**11b**, **12a**, and **12b**

Compound		H-1	H-2	H-3	H-4	H-5	Remaining signals
9a	δ_H	3.50	5.61	6.01	6.16	6.08	2.99 (Me), 3.43 (Me), 7.34–7.61 (5H, m, Ph)
	J	6.4	10.2	5.8	11.6		
10a	δ_H	7.30	5.45	2.43	5.26	5.92	3.03 (Me), 3.46 (Me), 7.34–7.61 (5H, m, Ph)
	J	9.5	6.8	6.8	9.7		
11a	δ_H	7.55	6.42	6.12	5.24	2.71	2.97 (Me), 3.43 (Me), 7.34–7.61 (5H, m, Ph)
	J	11.3	6.0	10.0	6.5		
9b	δ_H	3.38	5.62	6.03	6.41	6.70	3.39 (Me), 3.77 (Me), 3.81 (Me)
	J	6.5	10.1	7.4	11.5		
10b	δ_H	7.23	5.48	2.37	5.43	6.45	3.37 (Me), 3.77 (Me), 3.83 (Me)
	J	9.5	6.9	6.9	9.7		
11b	δ_H	7.48	6.40	6.14	5.38	3.02	3.39 (Me), 3.77 (Me), 3.83 (Me)
	J	11.2	6.0	10.0	6.6		
12a	δ_H	7.11	5.47	2.67	5.31	5.87	0.98 (Et), 2.94 (Me), 3.31 (Me), 2.72 (Et), 7.39–7.61 (5H, m, Ph)
	J	10.0	5.0	5.5	10.0		
12b	δ_H	7.05	5.47	2.53	5.51	6.51	1.02 (Et), 2.77 (Et), 3.11 (Et), 3.30 (Me), 3.77 (Me), 3.87 (Me)
	J	9.8	5.4	5.7	10.2		

concentration in vacuo. Satisfactory ^1H and ^{13}C NMR were obtained for **12a**,**b**; however, HRMS of **12b** gives only the $(M-NEt_2)^+$ peak instead of the M^+ peak. When compounds **12a**,**b** in the presence of diethylamine were kept for a few days in the dark, no change occurred. Upon treatment with aq. HBF_4 in Ac_2O, compounds **12a**,**b** regenerated **7a**,**b**·BF_4^- in good yield. Moreover, although the reactions of **7a**,**b**·BF_4^- with $PhCH_2OH$ or MeOH in the presence of K_2CO_3 were also monitored by NMR spectroscopy in CD_3CN, complex mixtures were obtained. Thus, the reaction sites of **7a**,**b**·BF_4^- with $PhCH_2OH$ and MeOH could not be determined.

2.3. Autorecycling oxidation of alcohols

We have previously reported that compounds **4**·BF_4^- and **5**·BF_4^- undergo autorecycling oxidation toward some alcohols under photo-irradiation.[12,14] In this context and in a search for the functions of **7a**,**b**·BF_4^-, we examined the oxidation of some alcohols by using **7a**,**b**·BF_4^- under aerobic and photo-irradiation conditions (RPR-100, 350 nm lamps). Although 1-phenylethanol was not oxidized by **7a**,**b**·BF_4^-, we found that compounds **7a**,**b**·BF_4^- have oxidizing ability toward benzylalcohol and cyclohexanol to give benzaldehyde and

Postulated mechanistic pathways for the present photo-induced oxidation of alcohols are depicted in Scheme 4.[12,14] The electron-transfer from alcohol to the excited cation **7a**,**b** generates a radical species **13a**,**b** and **14**, which react with molecular oxygen under photo-irradiation to afford a carbonyl compound, hydrogen peroxide, and original cation **7a**,**b** (Pathway A). The radical species **13a**,**b** would undergo

Table 5. Autorecycling oxidation of some alcohols by **7a**,**b**·BF_4^- under photo-irradiation

Entry	Additive	Alcohol	Carbonyl compound[a]	Yield[b] (%)
1	**7a**·BF_4^-	$PhCH_2OH$[c]	PhCHO	2420
2	**7b**·BF_4^-	$PhCH_2OH$[c]	PhCHO	1545
3	**7a**·BF_4^-	Cyclohexanol	Cyclohexanone	2351
4	**7b**·BF_4^-	Cyclohexanol	Cyclohexanone	961
5	**7a**·BF_4^-	PhCH(OH)Me	PhCOMe	0[d]
6	**7b**·BF_4^-	PhCH(OH)Me	PhCOMe	0[d]

CH_3CN solution was irradiated by RPR-100 350 nm lamps under aerobic conditions.

[a] Isolated as 2,4-dinitrophenylhydrazone.

[b] Based on **7a**,**b**·BF_4^- used; the yield, called 'blank', is subtracted from the total yield of carbonyl compound in the presence of **7a**,**b**·BF_4^-.

[c] In the presence of K_2CO_3 (1 mmol).

[d] The 'blank' yield was higher than the yield in the presence of **7a**,**b**·BF_4^-

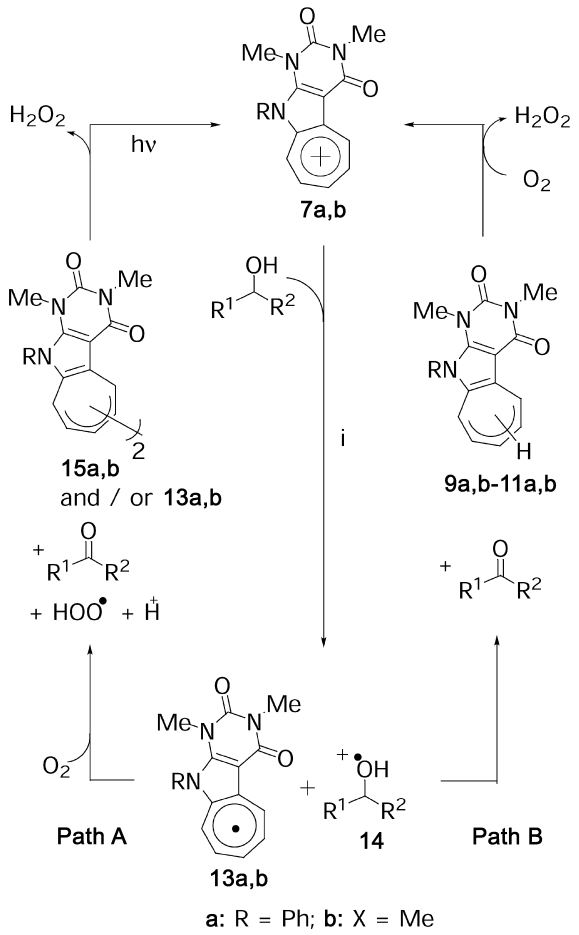

Scheme 4. *Reagents and conditions*: (i) CH_3CN, rt, aerobic, *hν*.

radical coupling to give dimers **15a**,**b**. This feature is suggested by the irreversible $E1_{red}$ of **7a**,**b** (vide supra). Since transformation of bitropyl into the corresponding tropylium ion by photo-induced electron transfer has been reported,[27] thus, the radical species **13a**,**b** as well as their dimers **15a**,**b** would be oxidized to regenerate cation **7a**,**b** under photo-irradiation and aerobic conditions. On the other hand, there is an alternative mechanistic pathway (Pathway B), in which compounds **9a**,**b**–**11a**,**b** in addition to the carbonyl compound are generated from **13a**,**b** and **14**; the former compounds are oxidized under aerobic conditions to regenerate **7a**,**b**. The reduced-products **9a**,**b**, **10a**,**b**, and **11a**,**b**, synthesized by reduction of **7a**,**b**·BF_4^- with $NaBH_4$, are also easily oxidized to give **7a**,**b**·BF_4^- under aerobic and photo-irradiation conditions in the presence of $NaBF_4$. Thus, autorecycling oxidation would also be possible in this Path B. Photo-irradiation of **7a**,**b**·BF_4^- and benzylalcohol in degassed CH_3CN resulted in a disappearance of **7a**,**b**·BF_4^- and the formation of a trace amount of benzaldehyde (detected by ^1H NMR), however, compounds **13a**,**b** or their dimers **15a**,**b** or compounds **9a**,**b**, **10a**,**b**, and **11a**,**b** could not be detected at the present stage. Thus, further investigations are required to clarify the mechanistic aspect of the reaction. The efficiency of autorecycling oxidation of alcohols with **7a**·BF_4^- (**7a**·BF_4^-, −0.84 V) seems to be higher as compared with that with **7b**·BF_4^- (**7b**·BF_4^-, −0.87 V) (Table 5, entries 1 vs. 2 and 3 vs. 4). Furthermore, the yields of the carbonyl compounds in the presence of **7a**,**b**·BF_4^- seem to be lower than those of **4**·BF_4^-[12] and **5**·BF_4^-[14] probably due to the more negative $E1_{red}$ values of **7a**,**b**·BF_4^- than those of **4**·BF_4^- (−0.58 V) and **5**·BF_4^- (−0.53 V). [The reduction potentials of **7a**,**b**·BF_4^- as well as **4**·BF_4^- and **5**·BF_4^- in the ground state would be correlated with their LUMO's, and thus, the LUMO's of these compounds would be lower in the order **7b**·BF_4^->**7a**·BF_4^->**4**·BF_4^->**5**·BF_4^-. In the excited state of these compounds, the electron-accepting orbital would be the singly occupied HOMO's. In as much as the UV–vis spectra of these compounds resemble each other, and the energy level of HOMO's of the compounds is expected to be lower in the order **7b**·BF_4^->**7a**·BF_4^->**4**·BF_4^->**5**·BF_4^-, and thus, the autorecycling oxidation of alcohols seems to be less efficient for **7a**,**b**·BF_4^- than for **4**·BF_4^- and **5**·BF_4^-.] In the oxidation reaction of benzylalcohol, the 'blank' yield in the absence of K_2CO_3 was higher than the yield in the presence of **7a**,**b**·BF_4^-. However, in the presence of K_2CO_3, the 'blank' yield became lower than the yield in the presence of **7a**,**b**·BF_4^- (Table 5, entries 1 and 2). While 5-deaza-10-oxaflavin **1b** possesses a strong function to oxidize alcohols in the absence of bases,[8] 5-deazaflavin **1a** oxidized alcohol in the presence of bases.[5] We have reported that compound **4**·BF_4^- oxidized di(1-phenylethyl) ether, but the rate of oxidation was much slower than that of 1-phenylethanol.[12] In the presence of K_2CO_3, the HBF_4–catalyzed formation of ether would be inhibited; however, no effect of K_2CO_3 was observed in the photo-induced oxidation reactions of cyclohexanol and 1-phenylethanol.

3. Conclusion

Convenient synthesis of 6-substituted 7,9-dimethylcyclohepta[*b*]pyrimido[5,4-*d*]pyrrole-8(7*H*),10(9*H*)-dionylium tetrafluoroborates **7a**,**b**·BF_4^-, which are nitrogen analogues of **4**·BF_4^- and **5**·BF_4^- as well as isoelectronic compounds of **1a**–**c** was accomplished. The structural characteristics of **7a**,**b**·BF_4^- were studied by the X-ray crystal analyses and MO calculations. The electronic properties of **7a**,**b**·BF_4^- were demonstrated by their UV–vis spectra, the pK_{R+} values, and the reduction potentials. A good linear correlation between the pK_{R+} values and reduction potentials ($E1_{red}$) of **7a**,**b**·BF_4^- as well as the reference compounds **4**·BF_4^- and **5**·BF_4^- was obtained. Moreover, reactions of **7a**,**b**·BF_4^- with some nucleophiles were demonstrated. Photo-induced autorecycling oxidation reaction of **7a**,**b**·BF_4^- toward some alcohols was carried out to afford the corresponding carbonyl compounds in yields of more than 100%. Further studies concerning the mechanistic aspect of the autorecycling oxidation would be required.

4. Experimental

4.1. General

IR spectra were recorded on a HORIBA FT-710 spectrometer. Mass spectra and high-resolution mass spectra were run on JMS-AUTOMASS 150 and JMS-SX102A spectrometers. ^1H NMR spectra and ^{13}C NMR spectra were recorded on a JNM-AL 400, a JNM-lambda 500, and an AVANCE 600 spectrometers, and the chemical shifts are given relative to internal $SiMe_4$ standard: *J*-values are given

in Hz. Mps were recorded on a Yamato MP-21 apparatus and were uncorrected. Compounds **2a**,**b** were prepared as described previously.[10]

4.2. Preparation of compounds 7a,b·BF_4^-

A mixture of **2a**,**b** (0.2 mmol) and MeI (1 cm^3) in CH_2ClCH_2Cl (5 cm^3) was placed in a sealed tube, and the mixture was heated at 120°C for 12 h. After evaporation of the solvent, the residue was dissolved in acetic anhydride (2.5 cm^3) and 42% aqueous HBF_4 (0.5 cm^3), and the mixture was stirred at 0°C for 1 h. To the mixture was added Et_2O (50 cm^3) and the precipitates were collected by filtration to give **7a**,**b**·BF_4^- (**7a**·BF_4^-, 79 mg, 98%; **7b**·BF_4^-, 57 mg, 83%).

4.2.1. 7,9-Dimethyl-6-phenylcyclohepta[*b*]pyrimido[5,4-*d*]pyrrole-8(7*H*),10(9*H*)-dionylium tetrafluoroborate (7a·BF_4^-). Yellow prisms; mp 250–251°C (from CH_3CN/Et_2O); ^{1}H NMR (500 MHz, CD_3CN) δ 3.14 (3H, s, Me), 3.48 (3H, s, Me), 7.70 (2H, d, J=8.2 Hz, *o*-Ph), 7.80 (2H, dd, J=8.2, 7.3 Hz, *m*-Ph), 7.87 (1H, t, J=7.3 Hz, *p*-Ph), 8.27 (1H, d, J=10.0 Hz, H-5), 8.37 (1H, dd, J=10.0, 9.7 Hz, H-4), 8.57 (1H, dd, J=9.8, 9.7 Hz, H-3), 8.65 (1H, dd, J=10.0, 9.8 Hz, H-2), 9.97 (1H, d, J=10.0 Hz, H-1); ^{13}C NMR (150.9 MHz) δ 29.0, 33.5, 99.2, 130.4, 131.8, 133.3, 134.1, 134.3, 139.8, 141.2, 143.3, 143.6, 145.8, 150.6, 152.0, 153.2, 158.9; IR (KBr) ν 1676, 1602, 1082 cm^{-1}; MS (FAB) *m*/*z* 318 (M^+-BF_4); HRMS calcd for $C_{19}H_{16}N_3O_2$: 318.1242 (M−BF_4). Found: 318.1277 (M^+-BF_4). Anal. calcd for $C_{19}H_{16}BF_4N_3O_2$: C, 56.33; H, 3.98; N, 10.37. Found: C, 56.1; H, 3.9; N, 10.3.

4.2.2. 6,7,9-Trimethylcyclohepta[*b*]pyrimido[5,4-*d*]pyrrole-8(7*H*),10(9*H*)-dionylium tetrafluoroborate (7b·BF_4^-). Yellow prisms; mp 232–233°C (from CH_3CN/Et_2O); ^{1}H NMR (400 MHz, CD_3CN) δ 3.41 (3H, s, Me), 3.94 (3H, s, Me), 4.34 (3H, s, Me), 8.46–8.58 (3H, m, H-2, 3, 4), 8.90–8.94 (1H, m, H-5), 9.84–9.89 (1H, m, H-1); ^{13}C NMR (150.9 MHz, CD_3CN) δ 28.9, 34.8, 36.2, 100.1, 132.7, 139.2, 140.5, 142.9, 143.2, 145.3, 149.4, 152.3, 154.2, 158.8; IR (KBr) ν 1696, 1588, 1084 cm^{-1}; MS (FAB) *m*/*z* 256 (M^+-BF_4); HRMS calcd for $C_{14}H_{14}BF_4N_3O_2$: 256.1086 (M−BF_4). Found: 256.1085 (M^+-BF_4). Anal. calcd for $C_{14}H_{14}BF_4N_3O_2$: C, 49.01; H, 4.11; N, 12.25. Found: C, 48.9; H, 3.7; N, 12.1.

4.3. Reaction of 7a,b·BF_4^- with $NaBH_4$

A solution of **7a**,**b**·BF_4^- (0.5 mmol) and $NaBH_4$ (19 mg, 0.5 mmol) in CH_3CN (10 mL) was stirred at rt for 1 h. To the mixture was added saturated aqueous NH_4Cl solution, and the mixture was extracted with CH_2Cl_2. The extract was dried over Na_2SO_4 and concentrated in vacuo to give mixtures of **9a**–**11a** and **9b**–**11b** (Table 3, entry 1, 2).

4.3.1. A mixture of 1,7-dihydro-7,9-dimethyl-6-phenylcyclohepta[*b*]pyrimido[5,4-*d*]pyrrole-8(7*H*),10(9*H*)-dione (9a), 3,7-dihydro-7,9-dimethyl-6-phenylcyclohepta[*b*]pyrimido[5,4-*d*]pyrrole-8(7*H*),10(9*H*)-dione (10a), and 5,7-dihydro-7,9-dimethyl-6-phenylcyclohepta[*b*]pyrimido[5,4-*d*]pyrrole-8(7*H*),10(9*H*)-dione (11a). Pale yellow powder, mp 202–203°C (from EtOH); IR (KBr) ν 1697, 1655 cm^{-1}; MS (FAB) *m*/*z* 319 (M^++H); HRMS calcd for $C_{19}H_{17}N_3O_2$: 319.1321 (M+H). Found: 319.1359 (M^++H). Anal. calcd for $C_{19}H_{17}N_3O_2$: C, 71.46; H, 5.37; N, 13.16. Found: C, 71.2; H, 5.4; N, 13.0.

4.3.2. A mixture of 1,7-dihydro-6,7,9-trimethylcyclohepta[*b*]pyrimido[5,4-*d*]pyrrole-8(7*H*),10(9*H*)-dione (9b), 3,7-dihydro-6,7,9-trimethylcyclohepta[*b*]pyrimido[5,4-*d*]pyrrole-8(7*H*),10(9*H*)-dione (10b), and 5,7-dihydro-6,7,9-trimethylcyclohepta[*b*]pyrimido[5,4-*d*]pyrrole-8(7*H*),10(9*H*)-dione (11b). Colorless powder, mp 185–186°C (from CH_2Cl_2/AcOEt); IR (KBr) ν 1692, 1648 cm^{-1}; MS (FAB) *m*/*z* 258 (M^++H); HRMS calcd for $C_{14}H_{15}N_3O_2$: 258.1243 (M+H). Found: 258.1250 (M^++H). Anal. calcd for $C_{14}H_{15}N_3O_2$ requires C, 65.36; H, 5.88; N, 16.33. Found: C, 64.8; H, 6.0; N, 16.0.

4.4. Oxidation of mixtures of 9a–11a and 9b–11b

To a stirred solution of a mixture of **9a**–**11a** or **9b**–**11b** (0.5 mmol) in CH_2Cl_2 (5 mL) was added DDQ (176 mg, 0.75 mmol), and the mixture was stirred at rt for 1 h. After evaporation of the CH_2Cl_2, the residue was dissolved in a mixture of acetic anhydride (5 mL) and 42% HBF_4 (1 mL) at 0°C, and the mixture was stirred for another 1 h. To the mixture was added Et_2O (50 mL) and the precipitates were collected by filtration to give **7a**,**b**·BF_4^- (Table 3).

4.5. ^{1}H NMR monitoring of reactions of 7a,b·BF_4^- with diethylamine

To the solutions of compounds **7a**,**b**·BF_4^- (0.01 mmol) in CD_3CN (0.5 mL) was added diethylamine (7.3 mg, 0.1 mmol) in a NMR tube. The NMR measurement was carried out immediately (after ca. 30 s).

4.5.1. 3-Diethylamino-3,7-dihydro-7,9-dimethyl-6-phenylcyclohepta[*b*]pyrimido[5,4-*d*]pyrrole-8(7*H*),10(9*H*)-dione (12a). ^{13}C NMR (150.9 MHz, CD_3CN) δ 13.5, 28.3, 33.1, 45.4, 61.7, 98.7, 115.3, 120.2, 121.4, 122.7, 123.1, 130.2, 130.7, 130.9, 134.8, 137.9, 140.9, 153.0, 160.2; MS (FAB) *m*/*z* 389 (M^++H); HRMS calcd for $C_{23}H_{26}N_4O_2$: 389.1978 (M+H). Found: 389.1998 (M^++H).

4.5.2. 3-Diethylamino-3,7-dihydro-6,7,9-trimethylcyclohepta[*b*]pyrimido[5,4-*d*]pyrrole-8(7*H*),10(9*H*)-dione (12b). ^{13}C NMR (150.9 MHz, CD_3CN) δ 13.3, 28.3, 33.4, 34.5, 45.3, 61.7, 98.3, 114.5, 120.2, 121.2, 122.3, 123.2, 134.1, 141.3, 153.2, 159.9; MS (FAB) *m*/*z* 256 (M−NEt_2); HRMS calcd for $C_{18}H_{24}N_4O_2$: 256.1086 (M−NEt_2). Found: 256.1064 (M−NEt_2).

4.6. Reaction of 12a,b with HBF_4

To solutions of **12a**,**b** (0.05 mmol) and diethylamine in CH_3CN, which were prepared by the reactions of **7a**,**b**·BF_4^- (0.05 mmol) with diethylamine (7.3 mg, 0.1 mmol) in CH_3CN (20 mL), were added a mixture of acetic anhydride (5 mL) and 42% aq. HBF_4 (1 mL) at 0°C. The mixtures were stirred for 1 h. To the mixture was added Et_2O (50 mL) and the precipitates were collected by filtration to give **7a**,**b**·BF_4^- (Table 3).

4.7. General procedure for autorecycling oxidation of alcohols catalyzed by 7a,b·BF_4^-

An CH_3CN (16 mL) solution of compound **7a**,**b**·BF_4^- (0.005 mmol) and alcohols (2.5 mmol, 500 equiv.) in the presence or absence of K_2CO_3 (138 mg, 1 mmol) in a Pyrex tube was irradiated by RPR-100 350 nm lamps under aerobic conditions for 16 h. The reaction mixture was concentrated in vacuo and diluted with ether and filtered. The filtrate was treated with a saturated solution of 2,4-dinitrophenylhydrazine in 2N HCl to give 2,4-dinitrophenylhydrazone. The results are summarized in Table 5.

4.8. X-Ray structure determination of 7a·BF_4^-†

Yellow prisms, $C_{19}H_{16}BF_4N_3O_2$, M=405.16, monoclinic, space group Cc, a=8.7681(4) Å, b=12.3225(8) Å, c=16.712(1) Å, β=91.122(1)°, V=1805.3(2) Å^3, Z=4, Dc=1.491 g cm^{-3}, crystal dimensions 0.60×0.60×0.20 mm^3. Data were measured on a Rigaku RAXIS-RAPID radiation diffractomater with graphite monochromated Mo Kα radiation. A total 7742 reflections were collected, using the ω-2θ scan technique to a maximum 2θ value of 55.0°. The structure was solved by direct methods and refined by a full-matrix least-squares method using SIR92 structure analysis software,[28] with 278 variables and 3409 observed reflections [$I>3.00\sigma(I)$]. The non-hydrogen atoms were refined anisotropically. The weighting scheme $w=[\sigma_c^2(F_0)+0.0030\times F_0^2]^{-1}$ gave satisfactory agreement analysis. The final R and Rw values were 0.034 and 0.062. The maximum peak and minimum peak in the final difference map were 0.39 and −0.39 e$^-$/Å^3.

4.9. X-Ray structure determination of 7b·BF_4^-†

Yellow prisms, $C_{14}H_{14}BF_4N_3O_2$, M=343.09, monoclinic, space group $P2_1/n$, a=7.664(3) Å, b=12.619(6) Å, c=15.129(6) Å, β=98.31(2)°, V=1447.7(1) Å^3, Z=4, Dc=1.574 g cm^{-3}, crystal dimensions 0.60×0.40×0.20 mm^3. Data were measured on a Rigaku RAXIS-RAPID radiation diffractomater with graphite monochromated Mo Kα radiation. A total 12666 reflections were collected, using the $\omega-2\theta$ scan technique to a maximum 2θ value of 55.0°. The structure was solved by direct methods and refined by a full-matrix least-squares method using SIR92 structure analysis software,[28] with 231 variables and 2069 observed reflections [$I>3.00\sigma(I)$]. The non-hydrogen atoms were refined anisotropically. The weighting scheme $w=[3.0000\times\sigma_c^2(F_0)+0.0010\times F_0^2+0.5000]^{-1}$ gave satisfactory agreement analysis. The final R and Rw values were 0.046 and 0.059. The maximum peak and minimum peak in the final difference map were 0.25 and −0.25e$^-$/Å^3.

4.10. Determination of pK_{R+} value of 7a,b·BF_4^-

Buffer solutions of slightly different acidities were prepared by mixing aqueous solutions of $Na_2B_4O_7$ (0.025 M) and HCl (0.1 M) (for pH 8.2–9.0), $Na_2B_4O_7$ (0.025 M) and NaOH (0.1 M) (for 9.2–10.8), Na_2HPO_4 (0.05 M) and NaOH (0.1 M) (for pH 11.0–12.0), and KCl (0.2 M) and NaOH (0.1 M) (for pH 12.0–14.0) in various portions. For the preparation of sample solutions, 1 cm^3 portions of the stock solution, prepared by dissolving 3–5 mg of cation **7a**,**b**·BF_4^- in MeCN (20 mL), were diluted to 10 cm^3 with the buffer solution (5 mL) and MeCN (4 mL). The UV–vis spectrum was recorded for each cation **7a**,**b** in 30 different buffer solutions. Immediately after recording the spectrum, the pH of each solution was determined on a pH meter calibrated with standard buffers. The observed absorbance at the specific absorption wavelengths (**7a**, 410 nm; **7b**, 414 nm) of each cation was plotted against pH to give a classical titration curve, whose midpoint was taken as the pK_{R+} value. The results are summarized in Table 2.

4.11. Cyclic voltammetry of cation 7a,b·BF_4^-

The reduction potentials of **7a**,**b**·BF_4^- were determined by means of CV-27 voltammetry controller (BAS Co). A three-electrode cell was used, consisting of Pt working and counter electrodes and a reference Ag/$AgNO_3$ electrode. Nitrogen was bubbled through a CH_3CN solution (4 mL) of each compound (0.5 mmol dm^{-3}) and Bu_4NClO_4 (0.1 mol dm^{-3}) to deaerate it. The measurements were made at a scan rate of 0.1 V s^{-1} and the voltammograms were recorded on a WX-1000-UM-019 (Graphtec Co) X-Y recorder. Immediately after the measurements, ferrocene (0.1 mmol) ($E_{1/2}$=+0.083) was added as the internal standard, and the observed peak potentials were corrected with reference to this standard. The compounds exhibited no reversible reduction wave: each of the reduction potentials was measured through independent scan, and they are summarized in Table 2.

† CCDC reference number 209501 (**7a**·BF_4^-) and 209502 (**7b**·BF_4^-).

Acknowledgements

Financial support from a Waseda University Grant for Special Research Project and 21COE 'Practical Nanochemistry' from MEXT, Japan is gratefully acknowledged. We thank the Materials Characterization Central Laboratory, Waseda University for technical assistance with the spectral data, elemental analyses and X-ray analysis.

References

1. Muller, F. *Chemistry and Biochemistry of Flavoenzymes*; Muller, F., Ed.; CRC: Boca Raton, 1991; Vol. 1, pp 1–71 and references cited therein.
2. Hamilton, G. A. *Progress in Bioorganic Chemistry*; Kaiser, E. T., Kezdy, F. J., Eds.; Wiley: New York, 1971; Vol. 1, p 83.
3. Brown, D. J. *Comprehensive Heterocyclic Chemistry*; Katritzky, A. R., Rees, C. W., Eds.; Pergamon, 1984; Vol. 3, pp 57–155.
4. Wamhoff, H.; Dzenis, J.; Hirota, K. *Adv. Heterocycl. Chem.* **1992**, *55*, 129–259.
5. Walsh, C. *Acc. Chem. Res.* **1986**, *19*, 216–221, and references cited therein.
6. Yoneda, F.; Tanaka, K. *Med. Res. Rev.* **1987**, *4*, 477–506, and references cited therein.
7. Yoneda, F.; Kokel, B. *Chemistry and Biochemistry of*

Flavoenzymes; Muller, F., Ed.; CRC: Boca Raton, 1991; Vol. 1, pp 121–169 and references cited therein.
8. Yoneda, F.; Hirayama, R.; Yamashita, M. *Chem. Lett.* **1980**, 1157–1160.
9. Yoneda, F.; Kawazoe, M.; Sakuma, Y. *Tetrahedron Lett.* **1978**, 2803–2806.
10. Nitta, M.; Tajima, Y. *Synthesis* **2000**, 651–654.
11. Takayasu, T.; Mizuta, Y.; Nitta, M. *Heterocycles* **2001**, *54*, 601–606.
12. Naya, S.; Miyama, H.; Yasu, K.; Takayasu, T.; Nitta, M. *Tetrahedron* **2003**, *59*, 1811–1821.
13. Naya, S.; Nitta, M. *Tetrahedron* **2003**, *59*, 3709–3718.
14. Naya, S.; Miyama, H.; Yasu, K.; Takayasu, T.; Nitta, M. *Tetrahedron* **2003**, *59*, 4929–4938.
15. Naya, S.; Nitta, M. *J. Chem. Soc., Perkin Trans. 1* **2000**, 2777–2781.
16. Naya, S.; Nitta, M. *J. Chem. Soc., Perkin Trans. 2* **2000**, 2427–2735.
17. Naya, S.; Nitta, M. *J. Chem. Soc., Perkin Trans. 2* **2001**, 275–281.
18. Naya, S.; Isobe, M.; Hano, Y.; Nitta, M. *J. Chem. Soc., Perkin Trans. 2* **2001**, 2253–2262.
19. Naya, S.; Nitta, M. *Tetrahedron* **2003**, *59*, 4157–4165.
20. Naya, S.; Sakakibara, T.; Nitta, M. *J. Chem. Soc., Perkin Trans. 2* **2001**, 1032–1037.
21. Mikata, Y.; Mizukami, K.; Hayashi, K.; Matsumoto, S.; Yano, S.; Yamazaki, N.; Ohno, A. *J. Org. Chem.* **2001**, *66*, 1590–1599.
22. Frisch, M. J.; Trucks, G. W.; Schlegel, H. B.; Scuseria, G. E.; Robb, M. A.; Cheeseman, J. R.; Zakrzewski, V. G.; Montgomery, J. A., Jr.; Stratmann, R. E.; Burant, J. C.; Dapprich, S.; Millam, J. M.; Daniels, A. D.; Kudin, K. N.; Strain, M. C.; Farkas, O.; Tomasi, J.; Barone, V.; Cossi, M.; Cammi, R.; Mennucci, B.; Pomelli, C.; Adamo, C.; Clifford, S.; Ochterski, J.; Petersson, G. A.; Ayala, P. Y.; Cui, Q.; Morokuma, K.; Salvador, P.; Dannenberg, J. J.; Malick, D. K.; Rabuck, A. D.; Raghavachari, K.; Foresman, J. B.; Cioslowski, J.; Ortiz, J. V.; Baboul, A. G.; Stefanov, B. B.; Liu, G.; Liashenko, A.; Piskorz, P.; Komaromi, I.; Gomperts, R.; Martin, R. L.; Fox, D. J.; Keith, T.; Al-Laham, M. A.; Peng, C. Y.; Nanayakkara, A.; Challacombe, M.; Gill, P. M. W.; Johnson, B.; Chen, W.; Wong, M. W.; Andres, J. L.; Gonzalez, C.; Head-Gordon, M.; Replogle, E. S.; Pople, J. A. *Gaussian98*, Revision A.11; Gaussian, Inc.: Pittsburgh PA, 2001.
23. Freedman, H. H. In *Carbonium Ions*; Olah, G. A., Schleyer, P., Eds.; Wiley-Insterscience: New York, 1973.
24. Okamoto, K.; Takeuchi, K.; Komatsu, K.; Kubota, Y.; Ohara, R.; Arima, M.; Takahashi, K.; Waki, Y.; Shirai, S. *Tetrahedron* **1983**, *39*, 4011–4024, and references cited therein.
25. (a) Doering, W.; von Knox, E. L. H. *J. Am. Chem. Soc.* **1954**, *76*, 3203–3206. (b) Doering, W.; von Knox, E. L. H. *J. Am. Chem. Soc.* **1957**, *79*, 352–356. (c) Okamoto, K.; Komatsu, K.; Kinoshita, T.; Shingu, H. *Bull. Chem. Soc. Jpn* **1970**, *43*, 1901–1902.
26. Viehe, H. G.; Merényi, R.; Stella, L.; Janousek, Z. *Angew. Chem. Int. Ed. Engl.* **1979**, *18*, 917–932, and references sited therein.
27. Jacobi, D.; Abraham, W.; Pischel, U.; Grubert, L.; Schnabel, W. *J. Chem. Soc., Perkin Trans 2* **1999**, 1241–1248.
28. Altomare, A.; Burla, M. C.; Camalli, M.; Cascarano, M.; Giacovazzo, C.; Guagliardi, A.; Polidori, G. *J. Appl. Crystallogr.* **1994**, *27*, 435.